JACS
JOURNAL OF THE AMERICAN CHEMICAL SOCIETY
Article
pubs.acs.org/JACS

CO Oxidation Promoted by Gold Atoms Supported on Titanium Oxide Cluster Anions

Xiao-Na Li,[†] Zhen Yuan,[†,‡] and Sheng-Gui He*,[†]

[†]Beijing National Laboratory for Molecular Sciences, State Key Laboratory for Structural Chemistry of Unstable and Stable Species, Institute of Chemistry, Chinese Academy of Sciences, Beijing 100190, People's Republic of China

[‡]University of Chinese Academy of Sciences, Beijing 100049, People's Republic of China

Supporting Information

ABSTRACT: Laser ablation generated $Au_x(TiO_2)_yO_z^-$ (x = 0, 1; y = 2, 3; z = 1, 2) oxide cluster anions have been mass-selected using a quadrupole mass filter and reacted with CO in a hexapole collision cell. The reactions have been characterized by time-of-flight mass spectrometry and density functional theory calculations. Gold−titanium bimetallic oxide clusters $Au(TiO_2)_yO_z^-$ are more reactive in CO oxidation than pure titanium oxide clusters $(TiO_2)_yO_z^-$. The computational studies identify the dual roles that the gold atom plays in CO oxidation: functioning as a CO trapper and electron acceptor. Both factors are important for the high reactivity of $Au(TiO_2)_yO_z^-$ clusters. To the best of our knowledge, this is the first example of CO oxidation by gold-containing heteronuclear oxide clusters, which provides molecular-level insights into the roles of gold in CO oxidation over oxide supports.

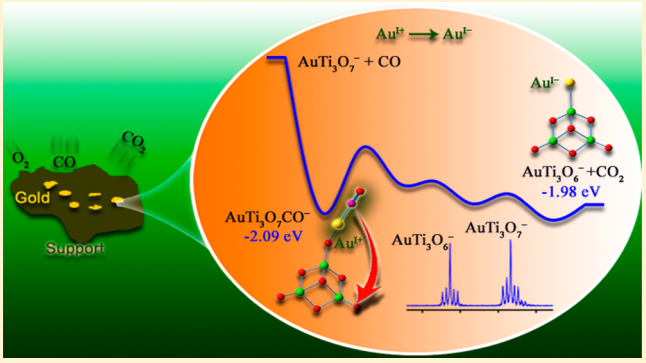

1. INTRODUCTION

The core of activity improvement of a particular catalyst is to get a clear structure−property understanding and an unambiguous identification of both the active sites and reaction mechanisms that govern the reactions. Highly dispersed gold exhibits extraordinary catalytic activity in CO oxidation at low temperatures, which has motivated extensive research activity since the breakthrough made by Haruta et al.[1] However, the contributions in this area have not reached a consensus on the nature of the active sites and reaction mechanisms. Some proposals emphasized the importance of cationic,[2] anionic,[3] zerovalent,[4] and low-coordinated gold centers.[5] Alternatively, some researchers attributed the activity to the perimeter sites between gold and the oxide support,[4b,6] and convincing evidence has pointed out the importance of the support as anchoring sites.[6a,7]

Study of gas-phase metal oxide clusters under isolated, controlled, and reproducible conditions is an important way to uncover the mechanistic details in related condensed-phase reactions.[8] The reactions of CO with $Au_x^{0,\pm}$ and $Au_xO_y^{\pm}$,[5a,9,10] $(TiO_2)_yO^-$ and $(ZrO_2)_yO^-$ (y = 1−25),[11] $Ce_xO_y^{\pm}$,[11c,12] Co_xO_y,[13] $Fe_xO_y^{0,\pm}$,[13b,14] and many others[8a,b,g−j,15] were extensively studied experimentally and theoretically. In general, CO can be oxidized by the atomic oxygen radical anion (O^-)[11,12,16] or CO can be first captured by the metal center and then oxidized by a nonradical oxygen atom (O^{2-}).[13,14c−g] In the CO oxidation by a $Au_2O_2^-$ cluster,[9a−c,e,10f] cooperative oxidation of two CO molecules was identified. CO oxidation by a few heteronuclear metal oxide clusters has also been reported,[17] and the available examples are $AlVO_4^+$,[17a] $VCoO_4$,[17b] and $YAlO_3^+$.[17c] In order to understand the nature of oxide-supported gold in CO oxidation, it is important to study gold-containing heteronuclear oxide clusters. The reaction of CO with gold−titanium oxide cluster cations was studied while only adsorption of CO was observed.[18] Thus, the important role that oxide-supported gold plays during the course of CO oxidation has not been determined from the viewpoint of cluster research. Furthermore, it is important to point out that most of the reported clusters that can oxidize CO are open-shell species and AuO^- anion is the only exception,[10b] to the best of our knowledge.

In this study, we report the first example of CO oxidation by closed-shell gold−titanium heteronuclear oxide cluster anions in an effort to understand CO oxidation on Au/TiO_2, which is a typical type of catalyst for efficient CO oxidation at low temperatures.[19]

2. METHODS

2.1. Experimental Methods. Details of the experimental setup can be found in previous studies,[16a,20] and only a brief outline of the experiments is given below. The $Au_x(TiO_2)_yO_z^-$ oxide cluster anions were generated by laser ablation of an Au/Ti mixed metal disk (1:1 Au:Ti molar ratio) in the presence of O_2 (0.2%) seeded in a He carrier gas (12 atm). The generated $Au_x(TiO_2)_yO_z^-$ oxide cluster anions were mass-selected using a quadrupole mass filter and reacted with pure CO or N_2 in a 80 mm long hexapole collision cell for about 40 μs with

Received: December 11, 2013
Published: February 14, 2014

   dx.doi.org/10.1021/ja412608b | J. Am. Chem. Soc. 2014, 136, 3617−3623

$(TiO_2)_yO_z^-$ clusters and for about 70 μs with $Au(TiO_2)_yO_z^-$ clusters. Before the prepared gases (pure CO, N_2, and O_2/He) were pulsed into the vacuum system, it was useful to pass them through copper tube coils at low temperature (~200 K, dry ice in ethanol) in order to remove a trace amount of water from the gas handling system. The intracluster vibrations were likely equilibrated to close to room temperature before reacting with CO.[16a,20] The reactant and product ions exiting from the reactor were detected by a reflection time-of-flight mass spectrometer (TOF-MS).[20a]

2.2. Theoretical Methods. Density functional theory (DFT) calculations with the hybrid B3LYP[21] functional and the Gaussian 09[22] program were performed to study the reaction mechanisms of $Au(TiO_2)_yO_z^-$ cluster anions with CO. A Fortran code based on a genetic algorithm (GA)[11e] was used to generate initial guess structures of $Au(TiO_2)_yO_z^-$ (y = 2, 3 and z = 1, 2) clusters. For each cluster, the smaller LANL2DZ basis sets[23] were adopted for all the atoms in the GA calculations that produced more than 200 optimized structures, among which more than 12 of the low-lying isomers were reoptimized by employing SDD basis sets[24] for Au and TZVP basis sets[25] for other atoms. This level of calculation has been tested to give reasonably good results for Au- and Ag-containing heteronuclear oxide clusters.[26] In the reaction mechanism calculations, the relaxed potential energy surface (PES) scan was used extensively to obtain good guess structures for the intermediates and the transition states (TS) along the reaction pathways. The TSs were optimized by using the Berny algorithm.[27] Intrinsic reaction coordinate calculations[28] were also performed so that each TS connects two appropriate local minima. Vibrational frequency calculations were carried out to check that reaction intermediates and TSs have zero and only one imaginary frequency, respectively. The basis set superposition error (BSSE) was calculated for the binding energies of a few $CO-Au(TiO_2)_yO_z^-$ complexes employing the counterpoise method.[29] The results indicated that the BSSE is negligible. The zero-point vibration corrected energies (ΔH_{0K}) without BSSE corrections are reported.

3. RESULTS

3.1. Experimental Results. The TOF mass spectra for the interactions of laser ablation generated and mass-selected $Au_x(TiO_2)_yO_z^-$ (x = 0, 1; y = 2, 3; z = 1, 2) cluster anions with CO are shown in Figure 1 and Figure S1 (Supporting Information). The interaction of $Ti_3O_7^-$ with CO produces a weak signal peak at the position of $Ti_3O_6^-$ (Figure 1b), which is consistent with our recent experiment that $(TiO_2)_yO^-$ (y = 3–25) cluster anions can oxidize CO to generate $(TiO_2)_y^-$ and CO_2 in a fast flow reactor.[11e] In contrast, the $AuTi_3O_7^-$ cluster anions produce a strong signal peak at the position of $AuTi_3O_6^-$ (Figure 1e) upon the interaction with CO, which indicates that one oxygen atom is transferred from $AuTi_3O_7^-$ to CO and produces $AuTi_3O_6^-$ and CO_2.

$$AuTi_3O_7^- + CO \rightarrow AuTi_3O_6^- + CO_2 \quad (1)$$

With N_2 as the reactant gas, the signals of $Ti_3O_6^-$ and $AuTi_3O_6^-$ are not observed within the experimental uncertainties (Figure 1c,f), indicating that these species are not the products of collision -induced dissociation. In addition, no product peak is observed upon the interaction of $Ti_3O_8^-$ with CO (Figure 1i), implying that the $Ti_3O_8^-$ cluster is inert toward CO oxidation. In contrast, the $AuTi_3O_8^-$ cluster is reactive and an apparent signal peak at the position of $AuTi_3O_7^-$ can be detected (Figure 1l):

$$AuTi_3O_8^- + CO \rightarrow AuTi_3O_7^- + CO_2 \quad (2)$$

Similar reactivity improvement is also observed upon the interactions of $AuTi_2O_5^-$ and $AuTi_2O_6^-$ with CO in comparison with those of $Ti_2O_5^-$ and $Ti_2O_6^-$ with CO (Figure S1, eqs 3 and 4). These experimental results clearly emphasize the importance of gold atom toward CO oxidation.

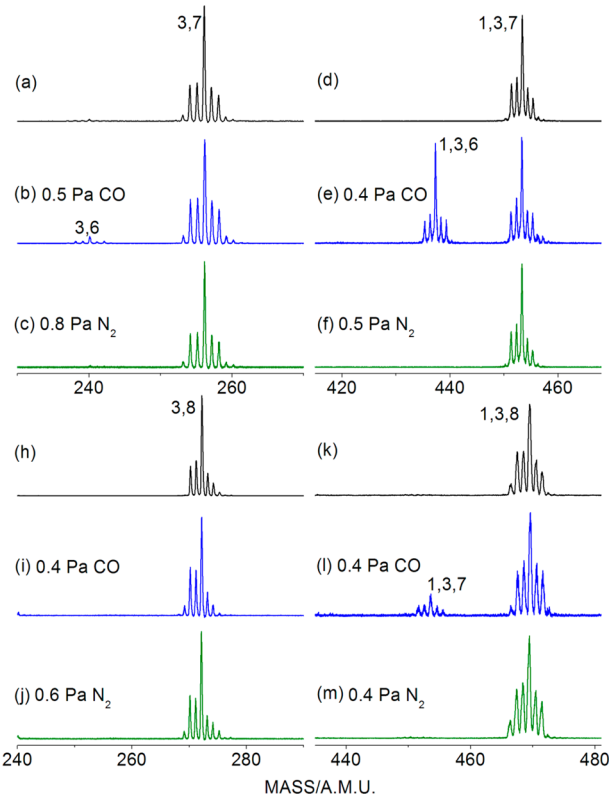

Figure 1. TOF mass spectra for reactions of mass-selected $Ti_3O_7^-$ (a–c), $AuTi_3O_7^-$ (d–f), $Ti_3O_8^-$ (h–j), and $AuTi_3O_8^-$ (k–m) with CO (b, e, i, and l) and N_2 (c, f, j, and m). The reference spectra without gas in the reactor are given in a, d, h, and k.

$$AuTi_2O_5^- + CO \rightarrow AuTi_2O_4^- + CO_2 \quad (3)$$

$$AuTi_2O_6^- + CO \rightarrow AuTi_2O_5^- + CO_2 \quad (4)$$

It should be noted that the adsorption of CO is not detected in our experiment for the cluster anions $Au(TiO_2)_yO_z^-$. This is different from the results in the reactions of $Au_xTi_yO_z^+$ cluster cations with CO, in which only CO adsorption was observed.[18] The pseudo-first-order rate constants (k_1) for the reactions between cluster ions and reactant molecules in the hexapole collision cell can be estimated by using the equation[20b,30]

$$k_1 = \ln[(I_R + I_P)/I_R]/(\rho \times \Delta t) \quad (5)$$

in which I_R and I_P are the signal intensities of the reactant ions and the product ions, respectively, ρ is the molecular density of the reactant gas, and Δt is the reaction time.[20b] The estimated rate constants are given in Table 1. The reaction of $AuTi_3O_7^-$ with CO (9.3×10^{-11} cm^3 molecule^{-1} s^{-1}) is much faster than that of $Ti_3O_7^-$ with CO (1.1×10^{-11} cm^3 molecule^{-1} s^{-1}). By using the hard-sphere[31] and classical[32] average dipole orientation (ADO) theories, the theoretical rate constants of collisions (k_{ADO}) between $Ti_3O_7^-$ and CO are both about 7.0×10^{-10} cm^3 molecule^{-1} s^{-1}. The reaction efficiency ($\Phi = k_1/k_{ADO}$) of $Ti_3O_7^-$ with CO is about 1.6%. Similarly, the reaction efficiency of $AuTi_3O_7^-$ with CO is about 9.5%.

dx.doi.org/10.1021/ja412608b | J. Am. Chem. Soc. 2014, 136, 3617–3623

Table 1. Pseudo-First-Order Rate Constants (k_1 in 10^{-11} cm^3 molecule^{-1} s^{-1}) for the Reactions of Clusters $Au_x(TiO_2)_yO_z^-$ (x = 0, 1; y = 2, 3; z = 1, 2) with CO

cluster	k_1	cluster	k_1
$Ti_3O_7^-$	1.1	$AuTi_3O_7^-$	9.3
$Ti_3O_8^-$		$AuTi_3O_8^-$	3.1
$Ti_2O_5^-$		$AuTi_2O_5^-$	0.6
$Ti_2O_6^-$		$AuTi_2O_6^-$	1.4

3.2. Theoretical Results. Aiming to provide insights into the mechanistic details of the remarkable reactivity of $Au(TiO_2)_yO_z^-$ cluster anions toward CO oxidation, the reaction pathways of $AuTi_3O_7^-$ + CO (Figure 2) and $AuTi_3O_8^-$ + CO (Figure S4, Supporting Information) are calculated on the singlet state PES (the corresponding triplet states are much higher in energy). The reaction pathway of $Ti_3O_7^-$ + CO has been reported in our recent study.[11e] The DFT calculated thermodynamic data for the reactions of $Ti_3O_7^-$, $AuTi_3O_7^-$, $Ti_3O_8^-$, and $AuTi_3O_8^-$ with CO are

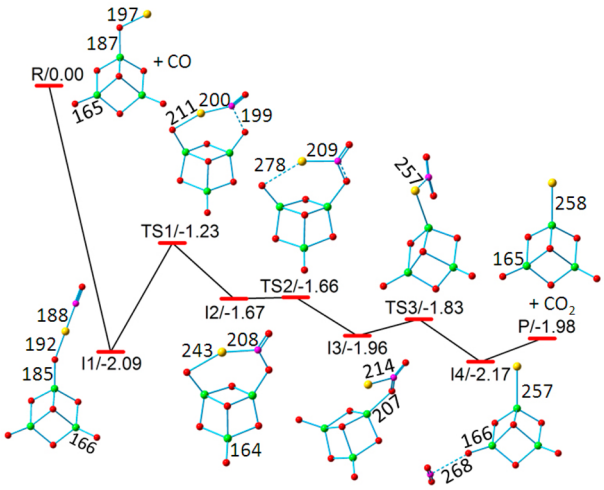

Figure 2. DFT calculated potential-energy profile for the reaction $AuTi_3O_7^-$ + CO → $AuTi_3O_6^-$ + CO_2. The zero-point vibration corrected energies (ΔH_{0K} in eV) of the reaction intermediates (I1−I4), transition states (TS1−TS3), and products (P: $AuTi_3O_6^-$ + CO_2) with respect to the separated reactants are given. Bond lengths are given in pm.

$$Ti_3O_7^- + CO \rightarrow Ti_3O_6^- + CO_2 \quad \Delta H_{0K} = -0.84 \text{ eV} \tag{5}$$

$$AuTi_3O_7^- + CO \rightarrow AuTi_3O_6^- + CO_2 \quad \Delta H_{0K} = -1.98 \text{ eV} \tag{6}$$

$$Ti_3O_8^- + CO \rightarrow Ti_3O_7^- + CO_2 \quad \Delta H_{0K} = -1.98 \text{ eV} \tag{7}$$

$$AuTi_3O_8^- + CO \rightarrow AuTi_3O_7^- + CO_2 \quad \Delta H_{0K} = -1.97 \text{ eV} \tag{8}$$

For the reaction of $Ti_3O_7^-$ with CO, the oxidation proceeds by an initial binding of the carbon atom of CO to the O^- radical in $Ti_3O_7^-$ (binding energy: ΔH_{0K} = 0.04 eV), and then the reaction is completed through the capture of the O^- radical to release CO_2.[11e] In contrast, CO is trapped tightly by the positively charged gold atom (natural charge: +0.468e) in $AuTi_3O_7^-$ at the first step (Figure 2). Natural bond orbital (NBO) analysis indicates that −0.057e negative charge is transferred from CO to $AuTi_3O_7^-$ upon CO adsorption, and a large energy is released in this process (I1 in Figure 2: ΔH_{0K} = −2.09 eV; ΔH_{0K} = −2.03 eV with BSSE correction).

After trapping of CO, the Au atom delivers CO to one of the terminal oxygen atoms to form a bent CO_2 unit (I2 in Figure 2, ΔH_{0K} = −1.67 eV). This step has an absolute barrier of 0.86 eV, which is the bottleneck of the whole reaction. The subsequent conversions proceed easily with negligible barriers. The whole reaction is barrierless overall, which is consistent with the experimental result. The reaction pathways without direct participation of the gold atom are also considered (Figure S3, Supporting Information). It turns out that these reaction pathways are subject to overall positive reaction barriers and are endothermic (ΔH_{0K} = 1.35 eV). Thus, reaction 1 must involve the direct participation of the gold atom (Figure 2). A similar mechanism shown in Figure S4 (Supporting Information) can be used to explain the high reactivity of $AuTi_3O_8^-$ toward CO oxidation (Figure 1l). The DFT calculated energetically low-lying isomers for the clusters $AuTi_3O_{6-8}^-$ and $AuTi_2O_{4-6}^-$ are plotted in Figures S5−S10 (Supporting Information). The correlation between the presence of the positively charged gold atoms and the enhanced cluster reactivity for $AuTi_2O_{5-6}^-$ versus $Ti_2O_{5,6}^-$ can also be found. The reactions between a few typical low-lying isomers of $AuTi_3O_{7-8}^-$ and CO have also been studied by DFT calculations (Figures S11−S14, Supporting Information). It turns out that the CO oxidation by these cluster isomers can follow the general mechanism shown in Figure 2 or Figure S4 (Supporting Information).

4. DISCUSSION

4.1. CO Trapper. The existence of specific sites for binding of reactants is thought to determine the reactivity of catalysts. The positively or negatively charged sites have a strong influence on the chemical and physical processes.[33] The adsorption of CO is sensitive to the charge environment of the reactive center. As a result, CO can be used as a probe molecule to detect the local charge distribution on particular systems.[34] The adsorption activity of CO has been extensively studied.[9b,d,35] It has been demonstrated that CO interacts strongly with positively rather than negatively charged species.[2b,4b]

The electrostatic potential maps (Figure 3a) indicate that the positively charged gold atom in $AuTi_3O_7^-$ functions as the preferred trapping site for CO adsorption (Figure 2). In contrast, the negatively charged O^- radical results in the formation of weakly bonded species.[11e] The lowest unoccupied molecular orbital (LUMO) of $AuTi_3O_7^-$ is mainly composed of the Au 6s orbital (55%, Figure 3b), which can overlap well with the highest occupied molecular orbital (HOMO) of CO. This rationalizes the fact of the large energy release upon CO adsorption. Furthermore, the good separation of the positive and negative charges within $AuTi_3O_7^-$ results in a very large dipole moment of 13.75 D. In contrast, the dipole moment of $Ti_3O_7^-$ is only 2.96 D. The higher dipole moment can lead to a local electric field and facilitate charge transfer,[36] which also contributes to the strong CO adsorption. The strong adsorption is important for a relatively higher efficiency of CO oxidation: Φ = 9.5% for the reaction $AuTi_3O_7^-$ + CO versus Φ =1.6% for the reaction $Ti_3O_7^-$ + CO.

dx.doi.org/10.1021/ja412608b | J. Am. Chem. Soc. 2014, 136, 3617−3623

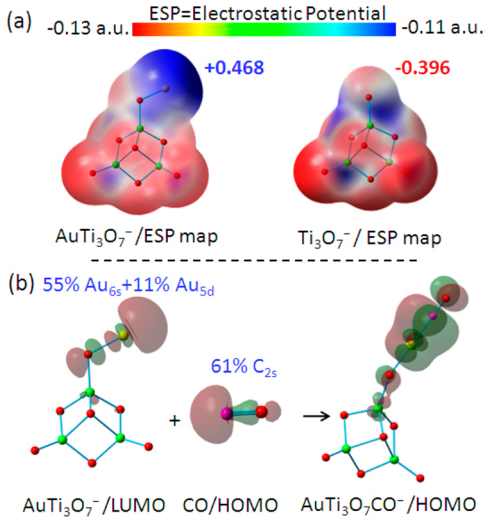

Figure 3. (a) Electrostatic potential maps for clusters $AuTi_3O_7^-$ and $Ti_3O_7^-$. Natural charges on Au^{I+} and O^- are given in e. (b) DFT calculated molecular orbitals for $AuTi_3O_7^-$ (LUMO), CO (HOMO), and $AuTi_3O_7CO^-$ (HOMO). 1 au = 27.2114 V.

4.2. Electron Acceptor. It is evident that the gold atom accumulates significant negative charge during the course of CO oxidation (Figure 4a). The oxidation states of the gold

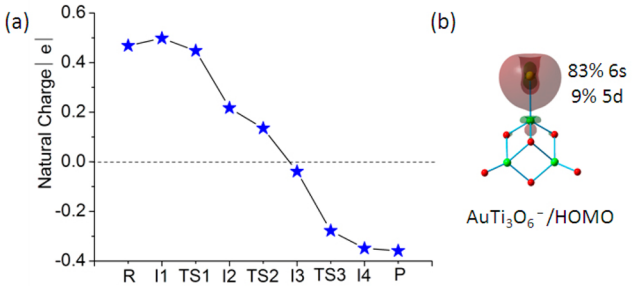

Figure 4. (a) Calculated natural charges (e) on the gold atom along the reaction pathway of $AuTi_3O_7^- + CO \rightarrow AuTi_3O_6^- + CO_2$ (see details in Figure 2). (b) HOMO of $AuTi_3O_6^-$.

atom change from positive (+0.468e) in $AuTi_3O_7^-$ to nearly neutral in I3 (of Figure 2) (−0.039e) and to negative (−0.359e) in $AuTi_3O_6^-$. The NBO analysis also indicates that the electronic configuration of the gold atom changes from [6s(0.77)5d(9.72)6p(0.01)] ($AuTi_3O_7^-$) to [6s(1.56)5d(9.81)-6p(0.01)] ($AuTi_3O_6^-$). This pronounced electron-trapping capability results from the strong relativistic effect in the gold system.[37] It is known that the gold atom has a contracted and stabilized 6s orbital, which tends to accept an electron.[37] The stored valence electrons in the Au−Ti bond are mainly localized on the Au 6s orbital (Figure 4b), which enhances the polarization interactions between Au and Ti and results in a strong Au−Ti bond (3.04 eV) of $AuTi_3O_6^-$. In contrast, the Au−O bond energy of $AuTi_3O_7^-$ is only 1.90 eV. It is noteworthy that $AuTi_3O_6^-$ is inert toward CO oxidation and CO can only be loosely connected at the negatively charged gold site (binding energy ΔH_{0K} = 0.03 eV; Figure S2 (Supporting Information)).

Charge transfer interactions between gold catalysts and metal oxide support are important in trapping the gold species,[38] and reductive[39] and oxidative[39,40] support environments are both confirmed to stabilize and activate gold. Thus, supported gold in different oxidation states (cationic, neutral, and anionic)[41] are often identified. Recently, we have reported the important role of gold as an electron acceptor in the reaction of $AuNbO_3^+$ with n-C_4H_{10},[26b] during which the gold atom changes its natural charge from +0.81e to +0.16e. Metal atoms can be in different cationic oxidation states during chemical reactions. For example, vanadium, cerium, and iron can change oxidation states as $V^{5+} \rightarrow V^{3+}$, $Ce^{4+} \rightarrow Ce^{3+}$, $Fe^{3+} \rightarrow Fe^{2+}$, and so on. However, the conversion of polarity (cationic → anionic) of metal oxidation states has never been identified in cluster reactions. Herein, we provide good experimental and theoretical evidence for the polarity conversion of metal oxidation states (Figure 4a, $Au^{I+} \rightarrow Au^{I-}$) during the course of CO oxidation for the first time.

4.3. Potential Electron Donor of Au^{I-}. CO oxidation on a bulk oxide surface may be divided into two steps: (1) oxidation of CO by the metal oxide, leaving a reduced oxide, and (2) oxidation of the reduced oxide by molecular oxygen. In this work, we mainly focus on the first step: CO oxidation. Superoxide (O_2^-) and peroxide (O_2^{2-}) have been identified to be active oxygen species in low-temperature CO oxidation over Au/TiO_2[42] and related systems.[43] In the gas-phase studies, the importance of the atomic oxygen radical O^- in CO oxidation has been identified.[11,12,16,17a,c] This study is among the first to report CO oxidation by gold-containing heteronuclear oxide clusters that are closed-shell species and do not have O^- radical centers. The strong CO-trapping and electron-accepting capabilities of gold guarantee the CO oxidation to proceed even more favorably than the CO oxidation by the O^- radical species.

The O_2 activation and O−O bond dissociation are also important in catalytic CO oxidation over oxide-supported gold. The activation of O_2 by the negatively charged gold (Au^{I-}) in the $AuTi_3O_6^-$ cluster is considered theoretically (Figures S15 and S16, Supporting Information). The O_2 activation is accompanied by electron flow into the $2\pi^*$ orbital, and the stored valence electrons in the Au−Ti bond can be released in this process ($Au^{I-} \rightarrow Au^{I+}$, Figure S16). The O_2 can be activated into a peroxide O_2^{2-} species (O−O bond 147 pm), and it may be not hard to overcome the 0.51 eV positive barrier (Figure S15) on the condensed-phase surfaces. The closed-shell $AuTi_3O_6^-$ cluster anion is a simple model, and a single gold anion (Au^{I-}) cannot provide enough electrons for further O−O bond dissociation ($O_2^{2-} \rightarrow O^{2-} + O^- \rightarrow 2O^{2-}$).

O_2 activation has attracted considerable attention experimentally and theoretically, and many important results have been obtained. For example, the odd−even alternation of reactivity in the reactions of gold cluster anions with O_2 was reported,[44] which arises from their alternating closed- and open-shell electronic structures. The closed-shell neutral gold cluster Au_8 can bind only weakly with an O_2 molecule, while its doped counterpart Au_7H has remarkable enhancement in binding with O_2.[45] The cooperative binding of CO + O_2[35c,d] and even O_2 + O_2 systems[46] was reported, in which the binding of the first molecule (CO or O_2) can change the electronic structure of the cluster and promote the approaching O_2 binding. Although most of these examples demonstrate activation of O_2 only to superoxide species (O_2^-, O−O bond ~131 pm), they provide important strategies to be considered in O−O bond dissociation by gold-containing heteronuclear oxide clusters. The simple model cluster $AuTi_3O_6^-$ can activate O_2 into peroxide O_2^{2-} species directly. The open-shell

dx.doi.org/10.1021/ja412608b | J. Am. Chem. Soc. 2014, 136, 3617−3623

electronic structures, doping of heteronuclear atoms, cooperative interactions, and the oxide-supported multiple Au^{I-} species may be important issues leading to complete O−O bond dissociation ($O_2^{2-} \rightarrow O^{2-} + O^- \rightarrow 2O^{2-}$).

The reaction mechanisms and the important roles of gold atom presented herein (Figures 2−4 and Figure S4) parallel the similar behaviors of the condensed phase systems studied by Widmann, Behm, and co-workers.[47] It was proposed that bulk TiO_2 supported Au nanoparticles (NPs) have two roles in the CO oxidation reaction: accumulate CO and activate the surface lattice oxygen close to the Au NPs. The highly stable surface lattice oxygen at the perimeter of the Au−TiO_2 interface can be removed by the reaction with CO through the proposed Au-assisted Mars−van Krevelen mechanism.[47b] This mechanism is well supported by the picture shown in Figure 2 or Figure S4 for the gas-phase cluster reactions: gold traps CO and delivers CO for oxidation by the "lattice" oxygen (O^{2-}) bonded to titanium. Furthermore, CO oxidation by FeO_x-[48] and CeO_2-supported[43a] gold catalysts may also follow a similar Au-assisted Mars−van Krevelen mechanism, which can be verified at the molecular level by studying the Au−Fe−O and Au−Ce−O clusters in the future.

It is noteworthy that the present study of CO oxidation with the cluster approach has the limitations of (1) small sizes of the clusters generated by the experiment and (2) short reaction time (40−70 μs) in the collision cell.[20b,49] Future developments will include generating and studying large Au−Ti−O cluster ions, particularly those with multiple gold atoms. An ion trap reactor that has the advantage of a long reaction time is under construction, and this equipment will be helpful to identify slow reactions and multistep reactions such as CO oxidation and then O_2 activation on atomic clusters. Our work on these topics is in progress.

5. CONCLUSION

In summary, we report the first example of CO oxidation by closed-shell gold-containing heteronuclear oxide clusters using mass spectrometry experiments and density functional theory calculations. The closed-shell cluster anions $AuTi_3O_8^-$, $AuTi_3O_7^-$, and $AuTi_2O_5^-$ are more reactive toward CO oxidation than the corresponding open-shell bare titanium oxide cluster anions $Ti_3O_8^-$, $Ti_3O_7^-$, and $Ti_2O_5^-$, among which $Ti_3O_7^-$ even contains an oxidative oxygen radical center. Theoretical calculations indicate that the gold atom plays dual roles in CO oxidation, functioning as a CO trapper and electron acceptor. Both factors are important for the high reactivity of $Au(TiO_2)_yO_z^-$ cluster anions. For the first time, a switch in the polarity of the metal oxidation state (cationic → anionic) during cluster reaction has been identified. The gas-phase reactions of $Au(TiO_2)_yO_z^-$ cluster anions with CO parallel similar behaviors of CO oxidation on bulk TiO_2-supported gold catalysts. This study provides molecular-level insights into the related surface reactions.

■ ASSOCIATED CONTENT

Supporting Information

Figures giving mass spectra, additional DFT calculation results, and natural charge distributions. This material is available free of charge via the Internet at http://pubs.acs.org.

■ AUTHOR INFORMATION

Corresponding Author

E-mail for S.-G.H.: shengguihe@iccas.ac.cn.

Notes

The authors declare no competing financial interest.

■ ACKNOWLEDGMENTS

This work was supported by the Major Research Plan of China (Nos. 2013CB834603 and 2011CB932302), the Natural Science Foundation of China (Nos. 21325314 and 21303215), and the ICCAS (No. CMS-PY-201306).

■ REFERENCES

(1) (a) Haruta, M. *Catal. Today* **1997**, *36*, 153−166. (b) Daté, M.; Haruta, M. *J. Catal.* **2001**, *201*, 221−224. (c) Liu, Z.-P.; Hu, P.; Alavi, A. *J. Am. Chem. Soc.* **2002**, *124*, 14770−14779.

(2) (a) Concepción, P.; Carrettin, S.; Corma, A. *Appl. Catal. A: Gen.* **2006**, *307*, 42−45. (b) Hutchings, G. J.; Hall, M. S.; Carley, A. F.; Landon, P.; Solsona, B. E.; Kiely, C. J.; Herzing, A.; Makkee, M.; Moulijn, J. A.; Overweg, A.; Fierro-Gonzalez, J. C.; Guzman, J.; Gates, B. C. *J. Catal.* **2006**, *242*, 71−81. (c) Wang, J. G.; Hammer, B. *Top. Catal.* **2007**, *44*, 49−56. (d) Fierro-Gonzalez, J. C.; Guzman, J.; Gates, B. C. *Top. Catal.* **2007**, *44*, 103−114.

(3) (a) Jansen, M. *Chem. Soc. Rev.* **2008**, *37*, 1826−1835. (b) Roldán, A.; Ricart, J. M.; Illas, F.; Pacchioni, G. *J. Phys. Chem. C* **2010**, *114*, 16973−16978.

(4) (a) Guzman, J.; Gates, B. C. *J. Phys. Chem. B* **2002**, *106*, 7659−7665. (b) Guzman, J.; Gates, B. C. *J. Am. Chem. Soc.* **2004**, *126*, 2672−2673.

(5) (a) Lopez, N.; Nørskov, J. K. *J. Am. Chem. Soc.* **2002**, *124*, 11262−11263. (b) Remediakis, I. N.; Lopez, N.; Nørskov, J. K. *Angew. Chem., Int. Ed.* **2005**, *44*, 1824−1826.

(6) (a) Liu, Z.-P.; Gong, X.-Q.; Kohanoff, J.; Sanchez, C.; Hu, P. *Phys. Rev. Lett.* **2003**, *91*, 266102. (b) Rodriguez, J. A.; Ma, S.; Liu, P.; Hrbek, J.; Evans, J.; Pérez, M. *Science* **2007**, *318*, 1757−1760.

(7) Green, I. X.; Tang, W.; Neurock, M.; Yates, J. T., Jr. *Science* **2011**, *333*, 736−739.

(8) (a) O'Hair, R. A. J.; Khairallah, G. N. *J. Cluster Sci.* **2004**, *15*, 331−363. (b) Böhme, D. K.; Schwarz, H. *Angew. Chem., Int. Ed.* **2005**, *44*, 2336−2354. (c) Schröder, D.; Schwarz, H. *Proc. Natl. Acad. Sci. U.S.A.* **2008**, *105*, 18114−18119. (d) Gong, Y.; Zhou, M.; Andrews, L. *Chem. Rev.* **2009**, *109*, 6765−6808. (e) Roithová, J.; Schröder, D. *Chem. Rev.* **2010**, *110*, 1170−1211. (f) Zhai, H.-J.; Wang, L.-S. *Chem. Phys. Lett.* **2010**, *500*, 185−195. (g) Castleman, A. W., Jr. *Catal. Lett.* **2011**, *141*, 1243−1253. (h) Zhao, Y.-X.; Wu, X.-N.; Ma, J.-B.; He, S.-G.; Ding, X.-L. *Phys. Chem. Chem. Phys.* **2011**, *13*, 1925−1938. (i) Yin, S.; Bernstein, E. R. *Int. J. Mass Spectrom.* **2012**, *321*−*322*, 49−65. (j) Lang, S. M.; Bernhardt, T. M. *Phys. Chem. Chem. Phys.* **2012**, *14*, 9255−9269. (k) Asmis, K. R. *Phys. Chem. Chem. Phys.* **2012**, *14*, 9270−9281.

(9) (a) Häkkinen, H.; Landman, U. *J. Am. Chem. Soc.* **2001**, *123*, 9704−9705. (b) Hagen, J.; Socaciu, L. D.; Elijazyfer, M.; Heiz, U.; Bernhardt, T. M.; Wöste, L. *Phys. Chem. Chem. Phys.* **2002**, *4*, 1707−1709. (c) Socaciu, L. D.; Hagen, J.; Bernhardt, T. M.; Wöste, L.; Heiz, U.; Häkkinen, H.; Landman, U. *J. Am. Chem. Soc.* **2003**, *125*, 10437−10445. (d) Veldeman, N.; Lievens, P.; Andersson, M. *J. Phys. Chem. A* **2005**, *109*, 11793−11801. (e) Tang, D. Y.; Zhang, Y. Q.; Hu, C. W. *Acta Chim. Sin.* **2008**, *66*, 1501−1507. (f) Prestianni, A.; Martorana, A.; Labat, F.; Ciofini, I.; Adamo, C. *J. Phys. Chem. C* **2008**, *112*, 18061−18066.

(10) (a) Wallace, W. T.; Whetten, R. L. *J. Am. Chem. Soc.* **2002**, *124*, 7499−7505. (b) Kimble, M. L.; Castleman, A. W., Jr.; Mitrić, R.; Bürgel, C.; Bonačić-Koutecký, V. *J. Am. Chem. Soc.* **2004**, *126*, 2526−2535. (c) Kimble, M. L.; Castleman, A. W., Jr. *Int. J. Mass Spectrom.* **2004**, *233*, 99−101. (d) Bernhardt, T. M.; Socaciu-Siebert, L. D.; Hagen, J.; Wöste, L. *Appl. Catal. A: Gen.* **2005**, *291*, 170−178. (e) Kimble, M. L.; Castleman, A. W., Jr.; Bürgel, C.; Bonačić-Koutecký, V. *Int. J. Mass Spectrom.* **2006**, *254*, 163−167. (f) Kimble, M. L.; Moore, N. A.; Johnson, G. E.; Castleman, A. W., Jr.; Bürgel, C.; Mitric, R.; Bonačić-Koutecký, V. *J. Chem. Phys.* **2006**, *125*, 204311. (g) Kimble, M. L.; Moore, N. A.; Castleman, A. W., Jr.; Bürgel, C.;

Mitrić, R.; Bonačić-Koutecký, V. *Eur. Phys. J. D* **2007**, *43*, 205−208. (h) Bürgel, C.; Reilly, N. M.; Johnson, G. E.; Mitrić, R.; Kimble, M. L.; Castleman, A. W., Jr.; Bonačić-Koutecký, V. *J. Am. Chem. Soc.* **2008**, *130*, 1694−1698. (i) Johnson, G. E.; Reilly, N. M.; Tyo, E. C.; Castleman, A. W., Jr. *J. Phys. Chem. C* **2008**, *112*, 9730−9736. (j) Popolan, D. M.; Bernhardt, T. M. *J. Chem. Phys.* **2011**, *134*, 091102.

(11) (a) Johnson, G. E.; Mitrić, R.; Tyo, E. C.; Bonačić-Koutecký, V.; Castleman, A. W., Jr. *J. Am. Chem. Soc.* **2008**, *130*, 13912−13920. (b) Johnson, G. E.; Mitrić, R.; Nössler, M.; Tyo, E. C.; Bonačić-Koutecký, V.; Castleman, A. W., Jr. *J. Am. Chem. Soc.* **2009**, *131*, 5460−5470. (c) Wu, X.-N.; Zhao, Y.-X.; Xue, W.; Wang, Z.-C.; He, S.-G.; Ding, X.-L. *Phys. Chem. Chem. Phys.* **2010**, *12*, 3984−3997. (d) Tyo, E. C.; Noler, M.; Mitric, R.; Bonačić-Koutecký, V.; Castleman, A. W., Jr. *Phys. Chem. Chem. Phys.* **2011**, *13*, 4243−4249. (e) Ma, J.-B.; Xu, B.; Meng, J.-H.; Wu, X.-N.; Ding, X.-L.; Li, X.-N.; He, S.-G. *J. Am. Chem. Soc.* **2013**, *135*, 2991−2998.

(12) Wu, X.-N.; Ding, X.-L.; Bai, S.-M.; Xu, B.; He, S.-G.; Shi, Q. *J. Phys. Chem. C* **2011**, *115*, 13329−13337.

(13) (a) Johnson, G. E.; Reveles, J. U.; Reilly, N. M.; Tyo, E. C.; Khanna, S. N.; Castleman, A. W., Jr. *J. Phys. Chem. A* **2008**, *112*, 11330−11340. (b) Reveles, J. U.; Johnson, G. E.; Khanna, S. N.; Castleman, A. W., Jr. *J. Phys. Chem. C* **2010**, *114*, 5438−5446. (c) Xie, Y.; Dong, F.; Heinbuch, S.; Rocca, J. J.; Bernstein, E. R. *Phys. Chem. Chem. Phys.* **2010**, *12*, 947−959.

(14) (a) Kappes, M. M.; Staley, R. H. *J. Am. Chem. Soc.* **1981**, *103*, 1286−1287. (b) Baranov, V.; Javahery, G.; Hopkinson, A. C.; Bohme, D. K. *J. Am. Chem. Soc.* **1995**, *117*, 12801−12809. (c) Blagojevic, V.; Orlova, G.; Bohme, D. K. *J. Am. Chem. Soc.* **2005**, *127*, 3545−3555. (d) Reilly, N. M.; Reveles, J. U.; Johnson, G. E.; Del Campo, J. M.; Khanna, S. N.; Köster, A. M.; Castleman, A. W., Jr. *J. Phys. Chem. C* **2007**, *111*, 19086−19097. (e) Reilly, N. M.; Reveles, J. U.; Johnson, G. E.; Khanna, S. N.; Castleman, A. W., Jr. *J. Phys. Chem. A* **2007**, *111*, 4158−4166. (f) Reilly, N. M.; Reveles, J. U.; Johnson, G. E.; Khanna, S. N.; Castleman, A. W., Jr. *Chem. Phys. Lett.* **2007**, *435*, 295−300. (g) Xue, W.; Wang, Z.-C.; He, S.-G.; Xie, Y.; Bernstein, E. R. *J. Am. Chem. Soc.* **2008**, *130*, 15879−15888.

(15) (a) Bernhardt, T. M. *Int. J. Mass Spectrom.* **2005**, *243*, 1−29. (b) Johnson, G. E.; Mitrić, R.; Bonačić-Koutecký, V.; Castleman, A. W., Jr. *Chem. Phys. Lett.* **2009**, *475*, 1−9. (c) Schlangen, M.; Schwarz, H. *Catal. Lett.* **2012**, *142*, 1265−1278.

(16) (a) Wu, X.-N.; Ma, J.-B.; Xu, B.; Zhao, Y.-X.; Ding, X.-L.; He, S.-G. *J. Phys. Chem. A* **2011**, *115*, 5238−5246. (b) Xu, B.; Zhao, Y.-X.; Ding, X.-L.; He, S.-G. *Int. J. Mass Spectrom.* **2013**, *334*, 1−7.

(17) (a) Wang, Z.-C.; Dietl, N.; Kretschmer, R.; Weiske, T.; Schlangen, M.; Schwarz, H. *Angew. Chem., Int. Ed.* **2011**, *50*, 12351−12354. (b) Wang, Z.-C.; Yin, S.; Bernstein, E. R. *J. Phys. Chem. Lett.* **2012**, 2415−2419. (c) Ma, J.-B.; Wang, Z.-C.; Schlangen, M.; He, S.-G.; Schwarz, H. *Angew. Chem., Int. Ed.* **2013**, *52*, 1226−1230.

(18) Himeno, H.; Miyajima, K.; Yasuike, T.; Mafuné, F. *J. Phys. Chem. A* **2011**, *115*, 11479−11485.

(19) Valden, M.; Lai, X.; Goodman, D. W. *Science* **1998**, *281*, 1647−1650.

(20) (a) Wu, X.-N.; Xu, B.; Meng, J.-H.; He, S.-G. *Int. J. Mass Spectrom.* **2012**, *310*, 57−64. (b) Yuan, Z.; Zhao, Y.-X.; Li, X.-N.; He, S.-G. *Int. J. Mass Spectrom.* **2013**, *354*−*355*, 105−112.

(21) (a) Lee, C.; Yang, W.; Parr, R. G. *Phys. Rev. B* **1988**, *37*, 785−789. (b) Becke, A. D. *J. Chem. Phys.* **1993**, *98*, 5648−5652.

(22) Frisch, M. J.; Trucks, G. W.; Schlegel, H. B.; Scuseria, G. E.; Robb, M. A.; Cheeseman, J. R.; Scalmani, G.; Barone, V.; Mennucci, B.; Petersson, G. A.; Nakatsuji, H.; Caricato, M.; Li, X.; Hratchian, H. P.; Izmaylov, A. F.; Bloino, J.; Zheng, G.; Sonnenberg, J. L.; Hada, M.; Ehara, M.; Toyota, K.; Fukuda, R.; Hasegawa, J.; Ishida, M.; Nakajima, T.; Honda, Y.; Kitao, O.; Nakai, H.; Vreven, T.; Montgomery, J. A., Jr.; Peralta, J. E.; Ogliaro, F.; Bearpark, M.; Heyd, J. J.; Brothers, E.; Kudin, K. N.; Staroverov, V. N.; Kobayashi, R.; Normand, J.; Raghavachari, K.; Rendell, A.; Burant, J. C.; Iyengar, S. S.; Tomasi, J.; Cossi, M.; Rega, N.; Millam, J. M.; Klene, M.; Knox, J. E.; Cross, J. B.; Bakken, V.; Adamo, C.; Jaramillo, J.; Gomperts, R.; Stratmann, R. E.; Yazyev, O.; Austin, A. J.; Cammi, R.; Pomelli, C.; Ochterski, J. W.; Martin, R. L.; Morokuma, K.; Zakrzewski, V. G.; Voth, G. A.; Salvador, P.; Dannenberg, J. J.; Dapprich, S.; Daniels, A. D.; Farkas, O.; Foresman, J. B.; Ortiz, J. V.; Cioslowski, J.; Fox, D. J. *Gaussian 09, Revision A.1*; Gaussian, Inc., Wallingford, CT, 2009; G09.

(23) Hay, P. J.; Wadt, W. R. *J. Chem. Phys.* **1985**, *82*, 270−283.

(24) Andrae, D.; Häußermann, U.; Dolg, M.; Stoll, H.; Preuß, H. *Theor. Chim. Acta* **1990**, *77*, 123−141.

(25) Schäfer, A.; Huber, C.; Ahlrichs, R. *J. Chem. Phys.* **1994**, *100*, 5829−5835.

(26) (a) Li, X.-N.; Wu, X.-N.; Ding, X.-L.; Xu, B.; He, S.-G. *Chem. Eur. J.* **2012**, *18*, 10998−11006. (b) Wu, X.-N.; Li, X.-N.; Ding, X.-L.; He, S.-G. *Angew. Chem., Int. Ed.* **2013**, *52*, 2444−2448.

(27) Schlegel, H. B. *J. Comput. Chem.* **1982**, *3*, 214−218.

(28) (a) Gonzalez, C.; Schlegel, H. B. *J. Chem. Phys.* **1989**, *90*, 2154−2161. (b) Gonzalez, C.; Schlegel, H. B. *J. Phys. Chem.* **1990**, *94*, 5523−5527.

(29) van Duijneveldt, F. B.; van Duijneveldt-van de Rijdt, J. G. C. M.; van Lenthe, J. H. *Chem. Rev.* **1994**, *94*, 1873−1885.

(30) Tian, L.-H.; Zhao, Y.-X.; Wu, X.-N.; Ding, X.-L.; He, S.-G.; Ma, T.-M. *ChemPhysChem* **2012**, *13*, 1282−1288.

(31) Kummerlöwe, G.; Beyer, M. K. *Int. J. Mass Spectrom.* **2005**, *244*, 84−90.

(32) (a) Su, T.; Bowers, M. *Int. J. Mass Spectrom. Ion Phys.* **1973**, *12*, 347−356. (b) Su, T.; Bowers, M. T. *J. Chem. Phys.* **1973**, *58*, 3027−3037. (c) Su, T.; Bowers, M. T. *J. Am. Soc. Chem.* **1973**, *95*, 1370−1373.

(33) Roldán, A.; Ricart, J. M.; Illas, F.; Pacchioni, G. *Phys. Chem. Chem. Phys.* **2010**, *12*, 10723−10729.

(34) (a) Sicolo, S.; Giordano, L.; Pacchioni, G. *J. Phys. Chem. C* **2009**, *113*, 10256−10263. (b) Lin, X.; Yang, B.; Benia, H.-M.; Myrach, P.; Yulikov, M.; Aumer, A.; Brown, M. A.; Sterrer, M.; Bondarchuk, O.; Kieseritzky, E.; Rocker, J.; Risse, T.; Gao, H.-J.; Nilius, N.; Freund, H.-J. *J. Am. Chem. Soc.* **2010**, *132*, 7745−7749.

(35) (a) Yuan, D. W.; Zeng, Z. *J. Chem. Phys.* **2004**, *120*, 6574−6584. (b) Fielicke, A.; von Helden, G.; Meijer, G.; Pedersen, D. B.; Simard, B.; Rayner, D. M. *J. Am. Chem. Soc.* **2005**, *127*, 8416−8423. (c) Prestianni, A.; Martorana, A.; Labat, F.; Ciofini, I.; Adamo, C. *J. Phys. Chem. B* **2006**, *110*, 12240−12248. (d) Amft, M.; Johansson, B.; Skorodumova, N. V. *J. Chem. Phys.* **2012**, *136*, 024312.

(36) Byun, Y.; Jeon, W. S.; Lee, T.-W.; Lyu, Y.-Y.; Chang, S.; Kwon, O.; Han, E.; Kim, H.; Kim, M.; Lee, H.-J.; Das, R. R. *Dalton Trans.* **2008**, 4732−4741.

(37) (a) Schwarz, H. *Angew. Chem., Int. Ed.* **2003**, *42*, 4442−4454. (b) Pyykkö, P. *Angew. Chem., Int. Ed.* **2004**, *43*, 4412−4456.

(38) Sanchez, A.; Abbet, S.; Heiz, U.; Schneider, W. D.; Häkkinen, H.; Barnett, R. N.; Landman, U. *J. Phys. Chem. A* **1999**, *103*, 9573−9578.

(39) Yu, X.; Wang, S.-G.; Li, Y.-W.; Wang, J.; Jiao, H. *J. Phys. Chem. C* **2012**, *116*, 10632−10638.

(40) Matthey, D.; Wang, J. G.; Wendt, S.; Matthiesen, J.; Schaub, R.; Laegsgaard, E.; Hammer, B.; Besenbacher, F. *Science* **2007**, *315*, 1692−1696.

(41) (a) Fierro-Gonzalez, J. C.; Gates, B. C. *Chem. Soc. Rev.* **2008**, *37*, 2127−2134. (b) Chen, M. S.; Goodman, D. W. *Chem. Soc. Rev.* **2008**, *37*, 1860−1870. (c) Coquet, R.; Howard, K. L.; Willock, D. J. *Chem. Soc. Rev.* **2008**, *37*, 2046−2076.

(42) Liu, H.; Kozlov, A. I.; Kozlova, A. P.; Shido, T.; Asakura, K.; Iwasawa, Y. *J. Catal.* **1999**, *185*, 252−264.

(43) (a) Carrettin, S.; Concepción, P.; Corma, A.; Nieto, J. M. L.; Puntes, V. F. *Angew. Chem., Int. Ed.* **2004**, *43*, 2538−2540. (b) Guzman, J.; Carrettin, S.; Fierro-Gonzalez, J. C.; Hao, Y. L.; Gates, B. C.; Corma, A. *Angew. Chem., Int. Ed.* **2005**, *44*, 4778−4781.

(44) Salisbury, B. E.; Wallace, W. T.; Whetten, R. L. *Chem. Phys.* **2000**, *262*, 131−141.

(45) Jena, N. K.; Chandrakumar, K. R. S.; Ghosh, S. K. *J. Phys. Chem. Lett.* **2011**, *2*, 1476−1480.

(46) Hagen, J.; Socaciu, L. D.; Le Roux, J.; Popolan, D.; Bernhardt, T. M.; Wöste, L.; Mitrić, R.; Noack, H.; Bonačić-Koutecký, V. *J. Am. Chem. Soc.* **2004**, *126*, 3442−3443.

(47) (a) Widmann, D.; Liu, Y.; Schüth, F.; Behm, R. J. *J. Catal.* **2010**, *276*, 292−305. (b) Widmann, D.; Behm, R. J. *Angew. Chem., Int. Ed.* **2011**, *50*, 10241−10245.
(48) Li, L.; Wang, A.; Qiao, B.; Lin, J.; Huang, Y.; Wang, X.; Zhang, T. *J. Catal.* **2013**, *299*, 90−100.
(49) Liu, Q.-Y.; He, S.-G. *Chem. J. Chinese U.* **2013**, DOI: 10.7503/cjcu20131066.